ARTICLES

(p,n) reaction on Li isotopes for $E_p = 60-200$ MeV

J. Rapaport
Physics Department, Ohio University, Athens, Ohio 45701

C. C. Foster and C. D. Goodman
Indiana University Cyclotron Facility, Bloomington, Indiana 47405

C. A. Goulding and T. N. Taddeucci
Los Alamos National Laboratory, Los Alamos, New Mexico 87545

D. J. Horen
Oak Ridge National Laboratory, Oak Ridge, Tennessee 37830

E. R. Sugarbaker
Physics Department, Ohio State University, Columbus, Ohio 43215

C. Gaarde and J. Larsen
Niels Bohr Institute, University of Copenhagen, DK 2100 Copenhagen, Denmark

J. A. Carr, F. Petrovich, and M. J. Threapleton
Physics Department and Supercomputer Computations Research Institute, The Florida State University, Tallahassee, Florida 32306

(Received 20 November 1989)

Differential cross section angular distributions for the ^{6,7}Li$(p,n)^{6,7}$Be reactions have been measured at energies between 60 and 200 MeV. The experimental angular distributions are analyzed using a microscopic distorted wave impulse approximation. The results of self-consistent microscopic distorted wave calculations based on a complete set of weak and electromagnetic data for the mass 6 and 7 systems are also presented. Total observed Gamow-Teller strength up to about 40 MeV excitation energy is reported. Energy dependence of the $\sigma\tau$ and τ effective interaction terms are presented up to 200 MeV. The measured (p,n) cross sections for the ^{7}Be (g.s.) and ^{7}Be (0.43 MeV) transitions are used to obtain the branching ratio of the ^{7}Be (g.s.) decay to the g.s. and 0.478 MeV states in ^{7}Li. Zero degree polarization transfer (D_{NN}) data at $E_p = 80$, 120, 160, and 200 MeV are reported for the ^{6}Li$(p,n)^6$Be (g.s.) and for the ^{7}Li$(p,n)^7$Be (g.s.$+0.43$ MeV) reactions. Energy dependence of total and zero degree differential cross section for the ^{7}Li$(p,n)^7$Be (g.s.$+0.43$ MeV) transitions are reported. Finally a comparison is presented for the (n,p), (p,p'), and (p,n) reaction in ^{6}Li populating isospin triplets.

I. INTRODUCTION

The (p,n) reactions on ^{6,7}Li have been extensively studied at incident proton energies below 50 MeV to obtain empirical values for the charge-exchange strength of the effective two-body interaction. Anderson, Wong and Madsen[1] proposed the comparison of the ^{7}Li$(p,n)^7$Be (g.s.) and ^{7}Li$(p,n)^7$Be (0.43 MeV) differential cross section values to deduce the ratio of the spin-isospin-dependent term of the effective interaction $V_{\sigma\tau}$, to the isospin-dependent term V_τ. Using nuclear structure information obtained from beta decay, the authors use the ratio of differential cross sections to obtain values of $(V_{\sigma\tau}/V_\tau)$ at bombarding energies below 20 MeV.[1] A similar analysis was used by Doering *et al.*[2] and Austin *et al.*[3] to extend the study to 45 MeV. Taddeucci *et al.*,[4] using a similar procedure, have extended this analysis up to 200 MeV. A consistent theoretical analysis of the charge-exchange data and inelastic proton scattering below 60 MeV incident proton energy has been reported by Petrovich *et al.*[5]

Other experimental studies of charge-exchange and proton elastic and inelastic scattering differential cross sections on ^{6,7}Li at intermediate energies have been carried out at the Indiana University Cyclotron Facility[6-9] (IUCF) and at TRIUMF.[10-12] In particular, the study of the ^{6}Li$(p,n)^6$Be reaction at 144 MeV has been reported by Moake *et al.*[6] as a test of one-pion exchange and the par-

tially conserved axial vector current. The scattering of 136 MeV protons from ^{6}Li has been reported by Henderson *et al.*[7] and the scattering of polarized protons from ^{6}Li and ^{7}Li at 200 MeV has been studied by Glover *et al.*[8] The 200 MeV data has been carefully analyzed in self-consistent distorted wave approximation calculations based on a realistic g-matrix interaction in which all available weak and electromagnetic data were used to constrain the nuclear structure input. The ^{6}Li$(n,p)^6$He (g.s.) reaction studied with 120 MeV neutrons is reported in Ref. 9. Results for the ^{6}Li$(n,p)^6$He (g.s.) at $E_n = 200$ MeV as a probe of Gamow-Teller strength are reported by Jackson *et al.*[10] and by Häusser[11] at 280 MeV; the latter also report on the ^{6}Li(p,p') at 280 MeV. Watson *et al.*[12] report on the ^{7}Li(p,n) cross section at 200, 300, and 400 MeV. Total reaction cross section for the ^{7}Li$(p,n)^7$Be (g.s. + 0.43 MeV) reaction in the energy range between 60 and 480 MeV has been presented in Refs. 13 and 14. In a recent paper, Taddeucci *et al.*[15] report zero degree cross sections for the ^{7}Li$(p,n)^7$Be (g.s. + 0.43 MeV) reaction in the energy range 80–790 MeV.

In the present study we present data for the ^{6,7}Li$(p,n)^{6,7}$Be reactions at incident energies between 60 and 200 MeV. Measured angular distributions are analyzed using a microscopic distorted wave impulse approximation (DWIA). The results obtained by extending the work of Ref. 8 to the present charge-exchange data are also given. We further discuss the spin-transfer data for the same energy region.

II. EXPERIMENTAL METHODS

The experiments were performed with the beam swinger neutron time-of-flight facility at the IUCF.[16] The experiments described here were done during a period of several years, and in several cases some of the measurements were repeated. Because of the large zero degree differential cross section to the ground-state (g.s.) transition, ^{7}Li is a target normally used to obtain absolute neutron detector efficiencies and neutron energy calibration. The zero degree differential cross section for the g.s. transition in the ^{6}Li$(p,n)^6$Be reaction is often used as a secondary standard to calibrate the experimental setup in (p,n) spin-transfer experiments.

Incident proton beam energies of 60, 80, 120, 160, and 200 MeV were used. Two neutron detector stations with path flights between 45–130 m and located outside the experimental hall were employed. One station was located along the 0° line with respect to an undeflected proton beam and the other was situated along the 24° line. Additional details about the experimental setup may be found in Ref. 16. Large volume time compensated plastic scintillators were located at the two neutron detector stations. Protons elastically scattered from the target were detected in fast plastic scintillators which provided ΔE and E information for particle identification. The output of this proton telescope was used in a phase compensation module[17] to eliminate long time drifts between the time of arrival of a beam burst on target and the radio frequency (rf) signal of the cyclotron. This time compensation was crucial for achieving subnanosecond resolution.

Self-supporting foils of ^{6}Li and ^{7}Li with enrichments greater than 99% and with thicknesses between 17 and 35 mg/cm^2 were used to measure the angular distributions. Similar foils, but generally 2–3 times thicker, were used to obtain the 0° yield of the reaction and the residual activity of the foil was measured to obtain the total reaction cross section. This was used to determine empirically the efficiency (including neutron attenuation in the flight path) and solid angle of the neutron detectors.[18] The electronics and data acquisition system used were similar to that described in Ref. 19.

Values from Ref. 14 for the ^{7}Li$(p,n)^7$Be (g.s. + 0.43 MeV) total cross section are used to evaluate the zero degree differential cross section needed in this normalization procedure. This normalization is about 14% smaller at 200 MeV, and about 6% smaller at 80 MeV than the values previously used by our group that employed total cross section values from Ref. 13. A more detailed study of the normalization procedure, extending the energy range up to 790 MeV, is presented in Ref. 15.

III. DATA AND RESULTS

Differential cross sections were measured over the angular range of $0° < \theta_{lab} < 50°$. The forward angle cross section data for transitions characterized with angular momentum transfer $L = 0$ were used to extrapolate the cross section to zero momentum transfer $q = 0$. The extrapolated cross section was expressed in units of Gamow-Teller strength B(GT) for those transitions with B(GT) values obtained from beta-decay lifetimes. Spin-transfer probabilities were measured only at 0°. In the next few paragraphs we will present data and results obtained for each Li isotope.

A. The ^{6}Li$(p,n)^6$Be reaction

Data were obtained at incident proton energies of 80, 120, 160, and 200 MeV. A zero degree spectrum for this reaction at 200 MeV (c.m. differential cross section versus outgoing neutron energy) is presented in Fig. 1(a). The dominant feature of the 0° spectra at all energies is the narrow peak at $Q = -5.1$ MeV. This corresponds to a transition to the ground state of ^{6}Be. The differential cross section peaks at 0° and has an $L = 0$ shape. Although this ground state is unbound to breakup into $\alpha + 2p$, it appears in nuclear reactions as a "state" with a width of about 90 keV.[20] In the (p,n) reaction we regard the peak as a Gamow-Teller transition that is the isospin mirror of the inverse beta decay of ^{6}He. No other forward-peaked narrow resonances are apparent in the spectrum. This point is of some interest because the possible existence of a narrow 0^+, $T = 1$ resonance in ^{6}Be at an excitation of about 11.5 MeV has been proposed[21,22] to explain the low flux of high-energy solar neutrinos. Other searches for this proposed resonance, Shopick *et al.*[23] and Fagg *et al.*,[24] find no evidence for such a resonance in electron scattering on ^{6}Li.

In our interpretation of the ^{6}Li$(p,n)^6$Be (g.s.) peak, the transition is driven by the spin-isospin term in the effective interaction. As pointed out in Refs. 25 and 26 this term of the effective interaction is almost energy in-

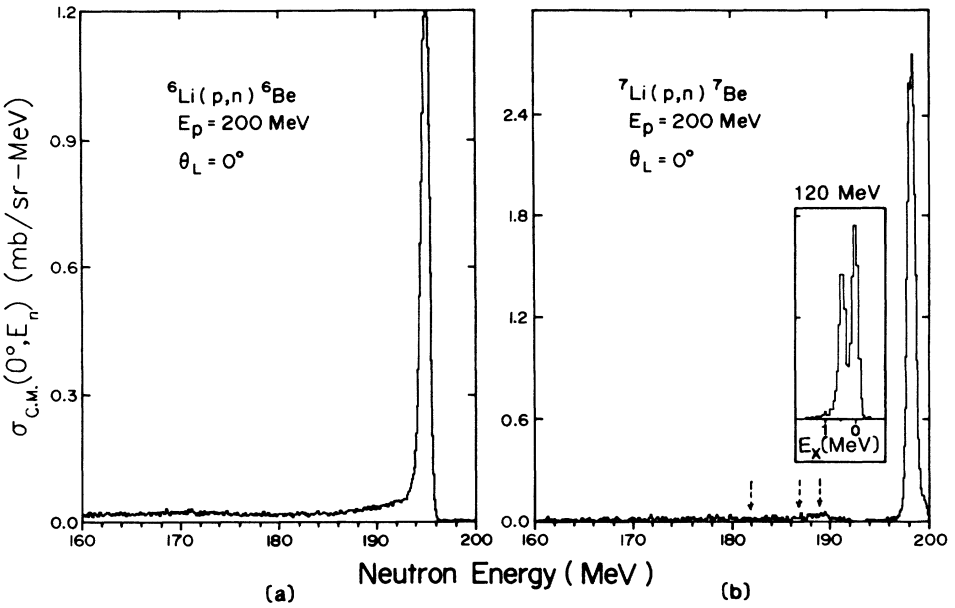

FIG. 1. (a) Neutron energy spectra at $E_p=200$ MeV and $\theta=0°$ for the ^{6}Li$(p,n)^6$Be reaction and (b) for the ^{7}Li$(p,n)^7$Be reaction. The inset shows transitions to the ^{7}Be (g.s.) and ^{7}Be (0.43 MeV) at $E_p=120$ MeV and $\theta=0°$. The dotted arrows in (b) indicate locations of weak transitions identified as Gamow-Teller transitions. Note the different scales for (a) and (b).

dependent between 100 and 200 MeV. We present in Fig. 2(a) values of the center-of-mass differential cross section at the measured energies plotted versus momentum transfer q. The fact that almost all data points cluster around a unique curve gives support to the above assumption. The variation in the distortion factor values[25] in this energy range is too small to be noticed.

B. The ^{7}Li$(p,n)^7$Be reaction

Data were obtained for this reaction at incident proton energies of 60, 80, 120, 160, and 200 MeV. A typical zero degree spectrum of differential cross section versus neutron energy at $E_p=200$ MeV, is presented in Fig. 1(b). The main feature of the 0° spectra at all energies is the ex-

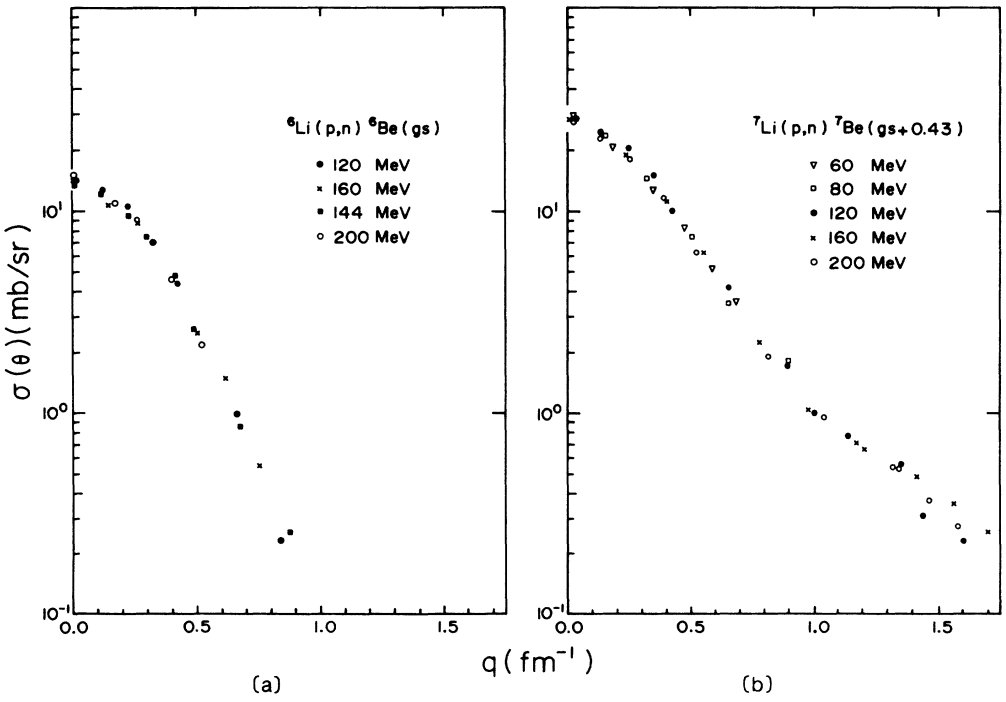

FIG. 2. Center-of-mass differential cross section for the ^{6}Li$(p,n)^6$Be (g.s.) transition and for the ^{7}Li$(p,n)^7$Be (g.s.+0.43 MeV) transition at the indicated proton energies plotted versus momentum transfer q.

citation of the g.s. and first excited (0.43 MeV) states. These states were resolved at all other energies. The inset in Fig. 1(b) shows a zero degree spectrum observed at $E_p = 120$ MeV. There are no particle-emission stable states in ^{7}Li above the first excited state.

The differential cross section for these two transitions peak at 0° and have $L = 0$ shapes. Shell model predictions for high lying states in ^{7}Be that may also be excited with angular momentum transfer $\Delta L = 0$ are rather limited. Norton and Goldhammer[27] suggest two $J^\pi = \frac{1}{2}^-$ levels with isospin $T = \frac{1}{2}$ at 11.3 and 12.5 MeV and a $J^\pi = \frac{3}{2}^-$ state with $T = \frac{1}{2}$ at 15.87 MeV. A $J^\pi = \frac{1}{2}^-$ level with $T = \frac{3}{2}$ is also predicted at 17.38 MeV. Cohen and Kurath[28] predict several states above 7.0 MeV excitation that carry a very small fraction of the total Gamow-Teller strength. From a phase shift analysis of the ^{3}He-^{4}He elastic scattering reaction and the R-matrix representation of the phenomenological phase shifts, Lui *et al.*[29] suggested the existence of a $J^\pi = \frac{1}{2}^-$ level at 16.7 MeV in ^{7}Be. The location of excited states in ^{7}Be at 9.9 MeV $(J^\pi, T = \frac{3}{2}^-, \frac{1}{2})$, 11.01 MeV $(J^\pi, T = \frac{3}{2}^-, \frac{3}{2})$, and 17 MeV $(J^\pi, T = \frac{1}{2}^-, \frac{1}{2})$ reported in Ref. 20 are indicated by the dotted lines in Fig. 1(b). Other states excited in the ^{7}Li$(p,n)^7$Be reaction were the 4.57 MeV $(J^\pi = \frac{7}{2}^-)$, 6.73 MeV $(J^\pi = \frac{5}{2}^-)$, and 7.21 MeV $(J^\pi = \frac{5}{2}^-)$ (Ref. 20), all excited with an angular distribution characterized with an $L = 2$ transfer that show a peak cross section at a momentum transfer $q \cong 0.9$ fm^{-1}. We do not present data for these transitions in this publication.

The ground-state transition $(\frac{3}{2}^- \rightarrow \frac{3}{2}^-)$ can include incoherent contributions from four amplitudes, $\Delta J^\pi = 0^+$ (Fermi), $\Delta J^\pi = 1^+$ (Gamow-Teller), $\Delta J^\pi = 2^+$ (quadrupole), and $\Delta J^\pi = 3^+$ (octupole). The 0.43 MeV state cross section $(\frac{3}{2}^- \rightarrow \frac{1}{2}^-)$ can include incoherent contributions from Gamow-Teller and quadrupole amplitudes. In Fig. 2(b) we present the sum of the center-of-mass differential cross sections for the two states plotted versus momentum transfer q. All data points cluster around a single curve, indicating that the shape of the differential cross sections does not depend on bombarding energy when plotted versus q.[12,15]

IV. ANALYSIS OF THE DATA AND DISCUSSION

The general approach in this paper is to compare the data with DWIA calculations using (i) the nuclear structure information given by free t-matrix interactions (DWIA) with beta decay information and Cohen and Kurath wave functions[28] (CKWF) and (ii) more realistic t-matrix interactions with nuclear structure information from beta decay and electromagnetic data as has been done in Ref. 8.

The code DWBA-70 (Ref. 30) was used for the microscopic DWIA calculations. In these calculations, the knockout exchange amplitude are treated exactly. Transition density amplitudes from CKWF were used assuming either harmonic oscillators (HO) or Woods-Saxon radial dependencies. Optical model parameters (OMP) for the distorted waves were obtained from proton elastic measurements on ^{6,7}Li, where available,[31–33] at the same incident energy or adjusted to the energy according to the appropriate energy dependence suggested in the $p + ^{12}$C analysis between 20–200 MeV by Comfort.[34] The choices of OMP made no more than a few percent changes in the calculations. Similarly, the use of HO or Woods-Saxon radial dependencies did not produce major changes into the calculations. We use the effective interaction as parametrized by Love and Franey.[35] We did not use a phenomenological 1-fm-range Yukawa interaction to parametrize the strength of the various components of the effective nucleon-nucleus interaction as was done for the analysis of (p,n) data at energies lower than 50 MeV.[1–3] Effects due to differences in ranges of the various components of the effective interaction as well as exchange effects play an important role in the calculations. A comparison of the energy dependence of the terms of the effective interaction obtained from the present analysis should be compared with care to prior results at lower energies.

Calculations at $E_p = 160$ MeV are compared with data in Fig. 3. For the ^{6}Li$(p,n)^6$Be (g.s.) transition, the HO potential size parameter had to be adjusted to a large value ($b = 2.15$ fm) to obtain the agreement shown in Fig. 3. No other variations in the input parameters were able to produce the observed agreement. A similar HO potential size parameter value is used in Ref. 11 to fit the ^{6}Li$(p,p')^6$Li (3.56 MeV) transition, analog to the ^{6}Li$(p,n)^6$Be (g.s.) transition. For ^{7}Li, the HO radial wave functions were calculated with an oscillator range parameter ($b = 1.73$ fm) obtained from fits[5] to the prominent maxima of the transverse form factors obtained in (e,e') experiments. The fits obtained with the CKWF deviate from the data for $q > 1.0$ fm^{-1} (Refs. 5 and 8), thus we expect that the present theoretical (p,n) results are inadequate beyond this momentum transfer. The sum of the calculated differential cross sections have been multiplied by a factor of 1.3 to obtain agreement with the data, as shown in Fig. 3 (see Sec. IV A).

The mass 6 and 7 systems have been extensively studied via the (e,e') reaction. A more realistic approach to the calculation of the (p,n) differential cross section is to base the calculations on transition densities deduced from the available weak and electromagnetic data. Such a study has recently been completed for the scattering of 200 MeV protons from ^{6,7}Li.[8] In that work, both the elastic and inelastic scattering are treated microscopically and self-consistently using the density-dependent g-matrix interaction based on the Paris potential[36,37] with exchange amplitudes treated approximately. These calculations have been extended to the present charge-exchange work and the theoretical results for the ^{6}Li$(p,n)^6$He (g.s.) and ^{7}Li$(p,n)^7$Be (g.s. + 0.43 MeV) transitions are compared with the 200 MeV data of this work in Fig. 4.

The agreement between these *parameter-free theoretical calculations* and experiment is good. It is important to note that the calculations predict the correct shape of the forward ^{6}Li$(p,n)^6$Be (g.s.) cross section. This is fixed from the ^{6}Li(e,e') data for the 1^+, $T = 0 \rightarrow 0^+$, $T = 1$ (3.56 MeV) transition. A better description of the backward angle ^{7}Li(p,n) data is also achieved. This is due almost

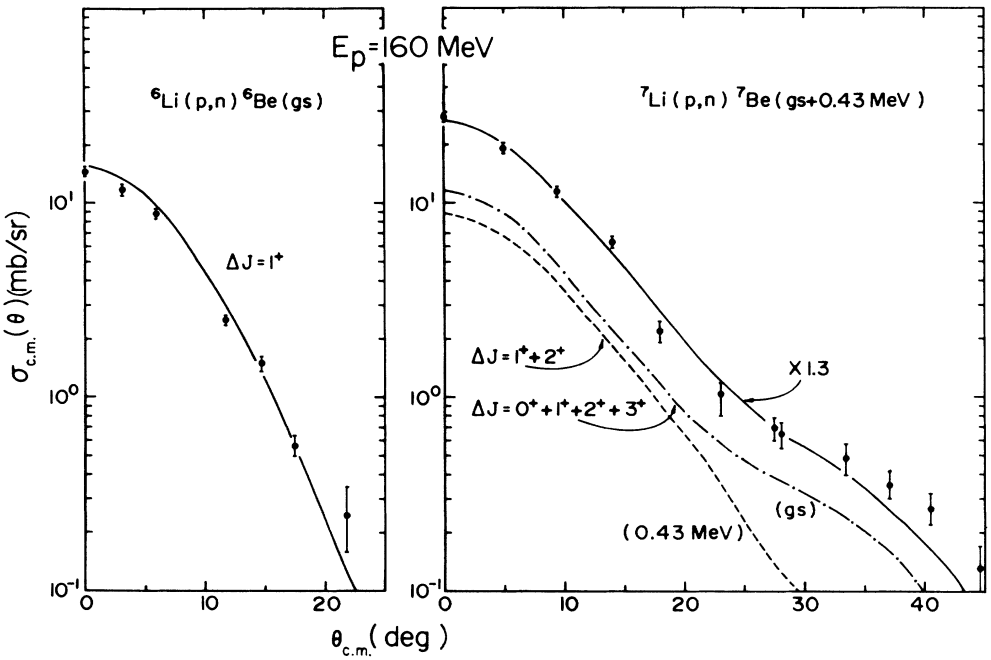

FIG. 3. Comparison between the measured differential cross section for the (p,n) g.s. transition in ^{6,7}Li at 160 MeV and DWIA calculated differential cross sections using CKWF (see text).

entirely to the $J^{\pi}=3^{+}$ contribution to the cross section, for which the ^{7}Li$(e,e')^{7}$Li transverse form factor data requires that the CKWF result be computed with $b=1.68$ fm and scaled by 1.10. The theoretical results in Fig. 4 slightly overpredict the ^{6}Li$(p,n)^{6}$Be (g.s.) cross section and slightly underpredict the ^{7}Li$(p,n)^{7}$Be (g.s.+0.43 MeV) cross section. This is the same as the relative normalization problem noted for the DWIA results shown in Fig. 3. The results in Fig. 4, due to the self-consistency imposed, clearly establish that the discrepancy is not associated with differences between densities or distortion effects in the mass 6 and 7 systems.

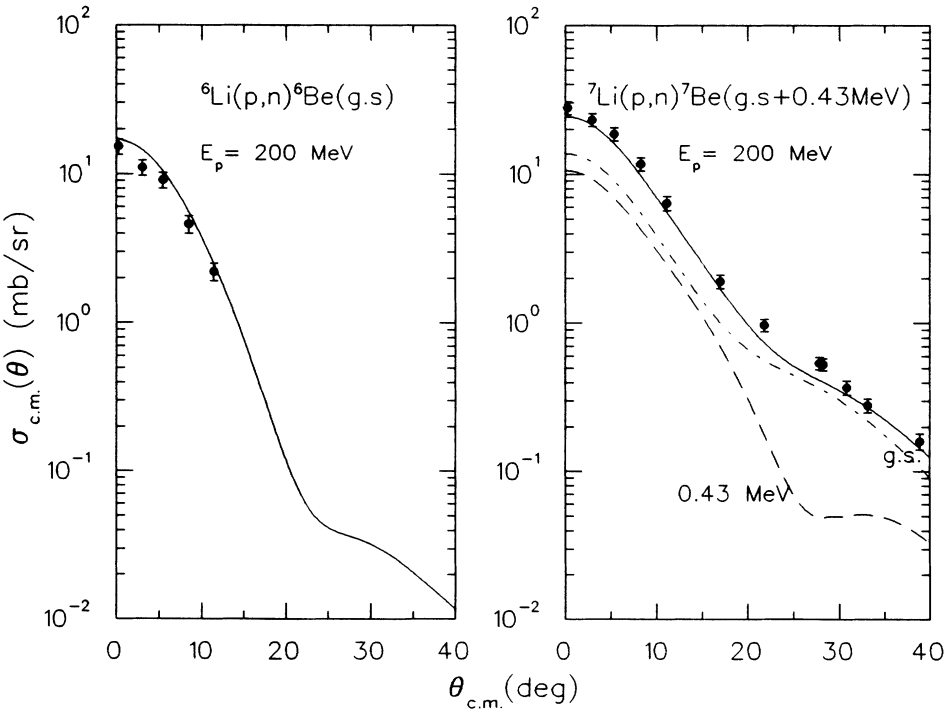

FIG. 4. Comparison between the measured differential cross section for the (p,n) g.s. transition in ^{6,7}Li at 200 MeV and DWIA calculations using transition densities deduced from the available weak and electromagnetic data (see text).

A. Gamow-Teller strength function

The zero degree spectrum is usually used to locate transitions characterized with an angular momentum transfer of $L=0$, and to estimate the GT strength distribution.[25,26] As reported in Refs. 38 and 39, the zero degree cross sections for these transitions may be factorized as[25,26,38,39]

$$\frac{d\sigma}{d\Omega}(q)=\left[\frac{\mu}{\pi\hbar^2}\right]^2\frac{k_f}{k_i}N_\alpha^D(q)|J_\alpha(q)|^2B(\alpha,q)\ , \tag{1}$$

where μ denotes the relativistic reduced energy divided by c^2 and k is the wave number; the index $\alpha=\sigma\tau(\tau)$ represents either a GT (spin-transfer) or a Fermi (non-spin-transfer) transition; the distortion factor N^D can be calculated;[25,26,38,39] $J_\alpha(q)$ represents the Fourier transform of the effective nucleon-nucleon interaction. At $q=0$, which roughly corresponds to $\theta=0°$ for the ^{6,7}Li$(p,n)^{6,7}$Be g.s. transitions, the nuclear structure factor $B(\alpha,q)$ becomes the reduced transition probability

$$B(\mathrm{GT})=\frac{1}{2J_i+1}|\langle f\|\sum_k\sigma_k t_k^-\|i\rangle|^2 \tag{2}$$

or

$$B(\mathrm{F})=\frac{1}{2J_i+1}|\langle f\|\sum_k t_k^-\|i\rangle|^2 \tag{3}$$

for the GT or Fermi transition.[25,26,38,39]

These reduced transition probabilities may be obtained directly from β-decay ft values according to the expression[39]

$$B(\mathrm{F})+\left[\frac{g_A}{g_V}\right]^2B(\mathrm{GT})=\frac{6616\pm2}{\mathrm{ft}}\ . \tag{4}$$

The value 6166±2 sec is essentially the vector coupling constant recommended by Wilkinson[40] while the quantity $(g_A/g_V)=1.260\pm0.008$ is the ratio of the axial to the vector coupling constant.[40] The factor f is the phase-space factor determined by the total energy release, and t is the half life for the β decay from the initial to the final state.

We have used the ft values tabulated in the compilations for $A=6$ (Ref. 41) and $A=7$ (Ref. 42) to calculate the B(GT) values for the g.s. transitions in ^{6,7}Li and the transition to the first excited state in ^{7}Be. These values are compared with the theoretical values predicted by the CKWF in Table I. Also shown in the table are the extrapolated experimental and theoretical $q=0$ differential cross sections per unit B(F), B(GT), i.e., $\hat{\sigma}_F$ or $\hat{\sigma}_{GT}$. We note that the B(GT) values obtained from β-decay ft values are smaller than the CKWF calculated values. We, therefore, make a first-order correction to the calculated DWIA cross section by scaling the calculated GT cross section by the ratio of measured B(GT) to the CKWF calculated B(GT).

In the case of the ^{6}Li$(p,n)^6$Be (g.s.) reaction, the solid curve shown in Fig. 3 includes the scaling factor 1.59/1.84=0.864 and shows a good overall agreement with the measured cross sections. The ^{6}Li$(p,n)^6$Be (g.s.) transition is the only transition that we observe to carry GT strength, up to an excitation energy of about 40 MeV. If there are other GT states, they may be very weakly excited or they may be very broad states and thus difficult to distinguish. The ratio between the experimental and CKWF calculated GT strength indicates that 86% of the predicted strength is concentrated in the g.s. transition.

Calculations for the ^{7}Li$(p,n)^7$Be (g.s.) transition involve the incoherent addition of differential cross sections calculated with $\Delta J^\pi=0^+$, 1^+, 2^+, and 3^+ amplitudes. We have scaled the $\Delta J^\pi=1^+$ (GT) component by the factor 1.24/1.62=0.764 and added it to the other CKWF calculated components, with the result indicated by the dotted-dashed curve in Fig. 3. For the ^{7}Be (0.43 MeV) state transition, the GT component is scaled by 1.11/1.33=0.835 and added to the calculated quadrupole contribution to give the dashed curve in Fig. 3. These scaled calculated curves still fall short of the data and need to be scaled by another factor of 1.3 to achieve agreement with the measurements, as shown in Fig. 3.

In the ^{7}Li$(p,n)^7$Be reaction some GT strength also appears to be present in weakly excited states in ^{7}Be at 9.9, 11.0, and 17 MeV [Fig. 1(b)]. We normalize the zero degree spectrum to the measured β decay values for the ground and first excited states to estimate upper limits of 0.02, 0.05, and 0.03 units for the GT strength in these transitions. The GT strength in these three excited states added to that of the g.s. and 0.43 MeV transitions (Table I) gives a total observed sum strength B(GT)=2.46. The sum CKWF calculated B(GT) strength amounts to 3.094. Thus the observed sum strength is about 80% of the theoretical values.

TABLE I. Structure information on transitions studied with (p,n) reactions.

Target	J_i,T_i	J_f,T_f	E_x MeV	B(GT) expt.[a]	CKWF	B(F)	$\hat{\sigma}_{GT}$ (mb/sr) (p,n) data[b]	$\hat{\sigma}_F$	$\hat{\sigma}_{GT}$ (mb/sr) DWIA[c]	$\hat{\sigma}_F$	$\hat{\sigma}_{GT}$ (mb/sr) g matrix[d]	$\hat{\sigma}_F$
^{6}Li	$1^+,0$	$0^+,1$	0.0	1.59±0.02	1.84		9.1		9.0		10.2	
^{7}Li	$\frac{3}{2}^-,\frac{1}{2}$	$\frac{3}{2}^-,\frac{1}{2}$	0.0	1.24±0.01	1.623	1.0	11.3	1.3	8.6	1.37	9.8	1.4
		$\frac{1}{2}^-,\frac{1}{2}$	0.43	1.11±0.05	1.331		11.4		8.0		9.5	

[a]From beta decay ft values (see text).
[b]Estimate uncertainty in $\hat{\sigma}_\alpha$ values is 10%; values at 160 MeV.
[c]Values at 160 MeV.
[d]Values at 200 MeV.

The 86% and 80% of the CKWF theoretical B(GT) values observed in the ^{6}Li$(p,n)^6$Be and ^{7}Li$(p,n)^7$Be reactions are similar to values obtained in other $1p$ nuclei.[43] However, for the ^{13}C$(p,n)^{13}$N and ^{15}N$(p,n)^{15}$O reactions, we have reported[44] that only about 40% of the predicted CKWF Gamow-Teller strength has been observed. This large discrepancy in the limit of observed GT strength may be due to the configuration mixing that become more important for nuclei near the end of a closed shell.[43] Another possible explanation[45] for this effect is due to different renormalizations required for the Gamow-Teller operator in the nuclear environment.

B. Energy dependence of the effective interaction

In Ref. 5, Taddeucci *et al.* present a study of the energy dependence of $J_{\sigma\tau}/J_\tau$. The motivation for the reported analysis was provided by the factorized DWIA expression for the $L=0(p,n)$ differential cross section, Eq. (1). The (p,n) reaction on even-A, nonzero isospin targets, leads to $0^+\rightarrow 1^+$ and $0^+\rightarrow 0^+$ transitions that are analogous to GT and F β decay, respectively. For such targets, the proportionality between the $q=0$ extrapolated (p,n) cross section and the corresponding β-decay strength suggests defining

$$|R(E_p)|^2=\frac{\sigma_{\rm GT}(q=0)/B({\rm GT})}{\sigma_{\rm F}(q=0)/B({\rm F})}\frac{K_{\rm GT}(E_p)}{K_{\rm F}(E_p)}=\frac{\hat{\sigma}_{\rm GT}}{\hat{\sigma}_{\rm F}}\frac{K_{\rm GT}(E_p)}{K_{\rm F}(E_p)}\ , \tag{5}$$

where $K(E_p)$ is just a kinematic factor, with a corresponding ratio very close to unity. This value $R(E_p)$ may also be interpreted as

$$|R(E_p)|=\left|\frac{J_{\sigma\tau}}{J_\tau}\right|\left[\frac{N_{\sigma\tau}}{N_\tau}\right]^{1/2}\ . \tag{6}$$

At energies below 200 MeV, the ratio of the distortion factors is close to unity and thus the value of $R(E_p)$ is a good representation of the energy dependence of the ratio of the two effective interactions. A value $R(E_p)=E_p$ (MeV)$/E_0$, with $E_0=55.0\pm0.4$ MeV, has been obtained[39] in the 50–200 MeV energy range. However, some anomalies have surfaced in this $R(E_p)$ value when comparing results in even-A targets with those of odd-A targets.[39,46]

The present data on ^{6,7}Li permit the study of the energy variation of the $\sigma\tau$- and τ-dependent terms in the effective interactions independently. The evaluation of $J_{\sigma\tau}$ and J_τ, or the ratio of these quantities from the data, assumes the exact validity of the factorization shown in Eq. (1). However, we know that they are only approximately valid,[39] and as indicated by Love *et al.*,[47] since J_τ is strongly energy and density dependent, we prefer instead to report on the energy dependence of the GT and F "unit cross sections" $\hat{\sigma}_\alpha$. This value is obtained by extrapolating to $q=0$ measured GT or F zero degree cross section and dividing it by the corresponding β-decay strength. Within the assumptions used for Eq. (1), we also may write

$$\sigma_\alpha=\hat{\sigma}_\alpha(A)F_\alpha(q,\omega)B(\alpha)\ , \tag{7}$$

where $F_\alpha(q,\omega)$ describes the momentum transfer q, and energy loss ω, dependence of the differential cross section. By definition $F_\alpha(q=0,\omega=0)=1$.

In Fig. 5 we present values for $\hat{\sigma}_{\rm GT}$ obtained from the ^{6}Li$(p,n)^6$Be (g.s.) and ^{7}Li$(p,n)^7$Be (0.43 MeV) transition. The F and GT contributions to the ^{7}Li$(p,n)^7$Be (g.s.) cross section were estimated as described in Ref. 39. These values were used to obtain the $\hat{\sigma}_{\rm F}$ and $\hat{\sigma}_{\rm GT}$ shown in Fig. 5. We also show values of $\hat{\sigma}_{\rm GT}$ obtained from the ^{12}C$(p,n)^{12}$N (g.s.) transition reported in Refs. 12 and 26. It is clear from the data that $\hat{\sigma}_{\rm GT}$ values for the ^{12}C and ^{6}Li targets (even A) show remarkably good agreement; the dashed line in Fig. 5 has been drawn at an energy constant value of $\hat{\sigma}_{\rm GT}=9.0$. The $\hat{\sigma}_{\rm GT}$ values obtained from ^{7}Li as a target (odd A) seem to be clustered at a value about 30% higher (dotted-dashed line). This is just the factor of 1.3 used to multiply the calculated DWIA values for the ^{7}Li$(p,n)^7$Be (g.s.+0.43) at 160 MeV to obtain agreement with the data (Fig. 3). In Fig. 5 we also show (solid line) the strong energy dependence displayed by $\hat{\sigma}_{\rm F}$ from data obtained from the ^{7}Li$(p,n)^7$Be (g.s.) transition.

Nakayama and Love[47] have calculated the energy dependence for zero degree ^{14}C$(p,n)^{14}$N cross sections to the F transition ($E_x=2.31$ MeV) and to the strong GT transition ($E_x=3.95$ MeV). The calculations were made using effective G-matrix interactions based on the Bonn and Paris potential as well as the SP84 t-matrix interaction. The calculated "unit cross sections" also indicate that $\hat{\sigma}_{\rm GT}$ remains constant in the 100–400 MeV energy

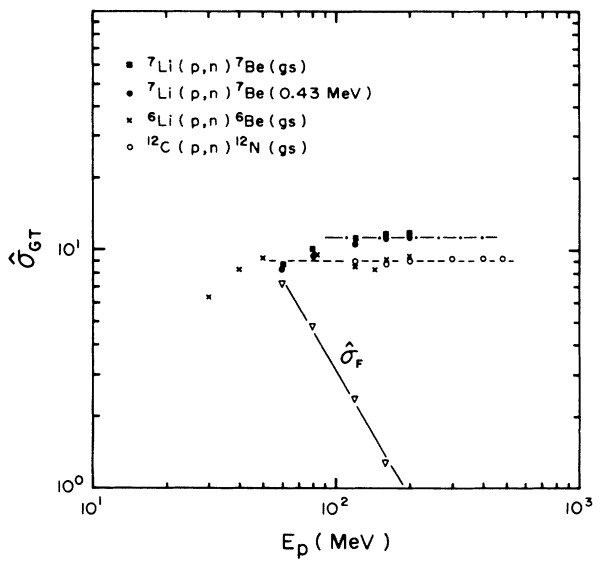

FIG. 5. Values of $\hat{\sigma}_{\rm GT}$ ($q=0$) for the ^{6}Li$(p,n)^6$Be (g.s.) and ^{12}C$(p,n)^{12}$N (g.s.) transitions at the indicated energies. Values for the $\hat{\sigma}_{\rm GT}$ ($q=0$) and $\hat{\sigma}_F$ ($q=0$) obtained from the ^{7}Li$(p,n)^7$Be (g.s.) and values for the $\hat{\sigma}_{\rm GT}$ ($q=0$) obtained from the ^{7}Li$(p,n)^7$Be (0.43 MeV) transition are also indicated. The indicated lines are drawn just to guide the eye.

interval and that $\hat{\sigma}_F$ decreases sharply between 100–200 MeV. These general results agree with the present data. For a discussion of the comparison of calculated and empirical "unit cross section ratios," see Ref. 48.

C. The ^{7}Be beta decay branching ratio

The accurate knowledge of the branching ratio in the electron-capture decay of ^{7}Be to the 478 keV and ground states of ^{7}Li has several important applications, among them the determination of the ^{3}He$(\alpha,\gamma)^7$Be cross section by activation techniques. The value of this cross section is an important parameter in the solar neutrino problem, defined as the discrepancy between the estimates of the neutrino flux from the sun reaching the earth based on the standard solar model and the measurements of the flux with the ^{37}Cl experiment.[49]

A measurement by Trautvetter *et al.*[50] of this branching ratio yielded a result of (15.4±0.8)%, almost 50% higher than the previously accepted value of (10.35 ±0.07)%.[42] This prompted several new measurements, which we do not present here and which are summarized and discussed by Skelton and Kavanagh.[51] In this section, we present an independent method to obtain this ratio, based on the proportionality between β-decay matrix elements and zero degree (p,n) cross sections discussed in the previous sections.

We define $\sigma_0(E)$ and $\sigma_1(E)$ as the measured zero degree cross sections for the ^{7}Li$(p,n)^7$Be reaction to the g.s. and 0.43 MeV states at incident energy E, respectively. Then we may write

$$\sigma_0(E)=\hat{\sigma}_{GT}(E)B^0(GT)+\hat{\sigma}_F(E)B(\mathrm{F}) \tag{8}$$

and

$$\sigma_1(E)=\hat{\sigma}_{GT}(E)B^1(\mathrm{GT})\ . \tag{9}$$

The GT matrix elements to the g.s. and 0.43 MeV state are denoted as B^0(GT) and B^1(GT), respectively. Thus the ratio of measured zero degree (p,n) cross sections may be written as

$$\frac{\sigma_0(E)}{\sigma_1(E)}=\frac{B^0(\mathrm{GT})+\dfrac{1}{R^2(E)}}{B^1(\mathrm{GT})}\ , \tag{10}$$

where $R(E_p)=(E_p/55)$ represents the ratio of GT to F zero degree cross section determined empirically from (p,n) measurements on several nuclei.[39] The value $B(\mathrm{F})=1.0$ has been implicitly used in Eq. (10).

Values for the ratio $\sigma_0(E)/\sigma_1(E)$, which are obtained from the measured zero degree cross sections at incident proton energy E, are very sensitive to the assumed B^0(GT) and B^1(GT) values. These GT strengths may be obtained from the β-decay adopted half-life value for the ^{7}Be (g.s.) decay and branching ratio value. The nucleus ^{7}Be decays only to the g.s. of ^{7}Li and to the 478 keV state in ^{7}Li.[20] To calculate the corresponding ft values, we use the adopted half-life $t_0=53.29\pm0.07d$ (Ref. 20) and the values of $\log_{10}f_0=-3.3885$ and $\log_{10}f_1=-4.1015$ (Ref. 52) for the g.s. and 0.48 MeV decay, respectively. We let the branching ratio vary between 8% and 15% to obtain

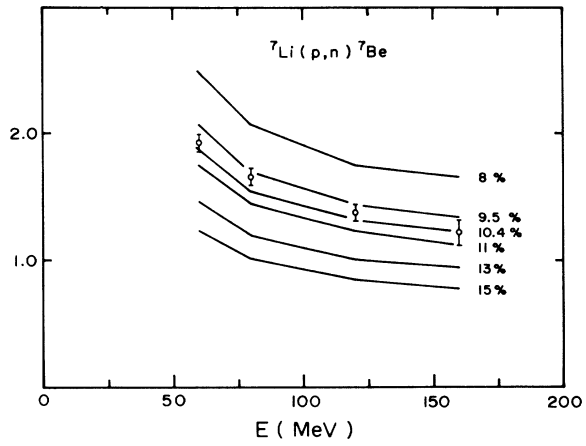

FIG. 6. Measured ratio for the zero degree ^{7}Li$(p,n)^7$Be (g.s.) and ^{7}Li$(p,n)^7$Be (0.43 MeV), σ_1, cross sections are compared with calculated ratios assuming the indicated branching ratio for the ^{7}Be (g.s.) β decay to the 0.48 MeV state in ^{7}Li.

calculated ft values. We use Eq. (4) to obtain the corresponding GT matrix element values which may be used in Eq. (10) to get calculated ratios for $\sigma_0(E)/\sigma_1(E)$. These are indicated in Fig. 6 as solid lines and are compared with the measured ratios at the indicated energies. It is clear from Fig. 6 that the measured values for the ratio of zero degree cross sections, $\sigma_0(E)/\sigma_1(E)$, are only compatible with a branching ratio of $(10.3^{+0.6}_{-1.0})\%$, in very good agreement with the (10.52±0.06)% recommended value.[20]

D. Polarization transfer measurements

Transverse polarization transfer in the direction perpendicular to the scattering plane has been measured for the ^{6}Li$(p,n)^6$Be (g.s.) and ^{7}Li$(p,n)^7$Be (g.s.+0.43 MeV) transitions in the bombarding energy range 80—200 MeV. In this case, the spin observables are related by

$$[1+p_i A(\theta)]p_f=P(\theta)+p_i D_{NN}(\theta)\ , \tag{11}$$

where p_i (p_f) is the incident (outgoing) nucleon polarization, $A(\theta)$ is the analyzing power for the reaction, P is the polarization function, and D_{NN} is the transverse spin-transfer coefficient. This coefficient is related to the transverse spin-flip probability by $D_{NN}=1-2S_{NN}$. At a scattering angle of 0°, the analyzing power and polarization are identical to zero, $A=P=0$, and the above equation becomes

$$p_f=p_i D_{NN}(0^\circ)\ . \tag{12}$$

Two parallel planes of plastic scintillators were used as polarization analyzers. They were located at $\theta=0°$ and at flight paths between 45–60 m. A complete description of the experimental arrangement has been published.[53]

We present in Fig. 7 $D_{NN}(0°)$ values for the ^{6}Li$(p,n)^6$Be (g.s.) transition. The data points (triangles) at 30 and 50 MeV are from Robertson *et al.*,[54] the data point (square) at 52.8 MeV is from Henneck *et al.*,[55] the 65 MeV data

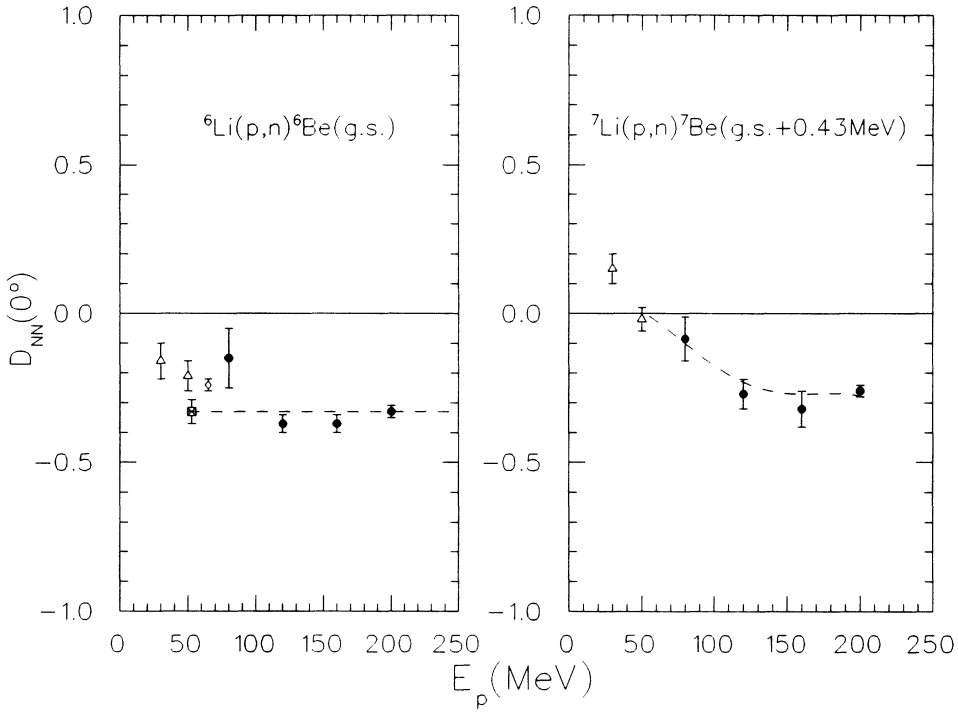

FIG. 7. Energy dependence of $D_{NN}(0°)$ for ^{6}Li$(p,n)^6$Be (g.s.) and ^{7}Li$(p,n)^7$Be (g.s.+0.43 MeV). The 30 and 50 MeV points (triangles) are from Ref. 53; the 52.8 MeV data point (square) is from Ref. 54; the 65 MeV point (diamond) is from Ref. 55. The solid circles are from this work; the dotted line represents PWIA values (see text).

point (diamond) is from Sakai *et al.*,[56] and the solid circles at 80, 120, 160, and 200 MeV are from this work. The plane wave impulse approximation (PWIA) has been shown[57] to provide a convenient means of predicting D_{NN} values. If the spin term of the interaction can be represented simply as $\sigma_1 \cdot \sigma_2$, as in the case of a pure GT transition, then $D_{NN} = -\frac{1}{3}$. This value is represented by the dashed line in Fig. 7. These results have been tested with DWIA calculations[57] including realistic effective interactions and knockon exchange amplitudes, showing good agreement with the above values in this energy range, 80–200 MeV. The theoretical calculations producing the 200 MeV results for the ^{6}Li$(p,n)^6$Be (g.s.) transition shown in Fig. 4 give a value $D_{NN}(0°) = -0.26$.

The $D_{NN}(0°)$ values for the ^{7}Li$(p,n)^7$Be (g.s.+0.43 MeV) transitions are also presented in Fig. 7 at 30 and 50 MeV (triangles) from Ref. 54, and 80, 120, 160, and 200 MeV (solid circles) data points from this work. In this case the g.s. transition has a Fermi component which is totally spin independent and thus with $D_{NN} = 1$. The dashed line represents the values expected if $D_{NN} = -\frac{1}{3}$ for the GT component and the ratio of GT and F cross sections evaluated as indicated in Sec. IV C. The theoretical calculations at 200 MeV shown in Fig. 4 give a value $D_{NN}(0°) = -0.16$ for these two transitions.

E. Energy dependence of total and zero degree differential cross sections

Total cross sections (σ_T) for the ^{7}Li$(p,n)^7$Be (g.s.+0.43 MeV) reactions have been reported using activation techniques by D'Auria *et al.*[14] The data between 60 and 480 MeV incident proton energies seem to be well represented by the equation

$$\ln\sigma(E) = -1.13 \ln E_p + 7.05 , \tag{13}$$

where E_p is the lab energy in MeV and $\sigma(E)$ is the total cross section in mb. The data of Ref. 14 (circles) are presented in Fig. 8 with data points for energies less than 50 MeV, represented as triangles, selected from references mentioned in Ref. 58 (see also Refs. 15 and 39). For comparison we also present in Fig. 8 (solid squares) values obtained from DWIA calculations for the total cross section obtained using CKWF and Love and Franey[35] interactions. The dashed-dotted line in the 20–150 MeV energy range represent values obtained for the total free *n-p* elastic cross section obtained from the VPI@SU SAID solution SM89.[59] Above 150 MeV the solid circles represent the total free *n-p* cross section. These values, presented in Fig. 8, have been divided by 10. Up to about 150 MeV proton lab energy, the total free *n-p* elastic cross section, which is almost identical to the total free *n-p* cross section, may be represented by the equation

$$\ln\sigma(E) = -1.13 \ln E_p + 9.55 \tag{14}$$

with identical energy coefficient to Eq. (13) and thus parallel to the line representing the ^{7}Li$(p,n)^7$Be (g.s.+0.43 MeV) total cross section. A theoretical interpretation of the $1/E$ dependence of the ^{7}Li$(p,n)^7$Be (g.s.+0.43 MeV) total reaction cross section is presented in Ref. 13.

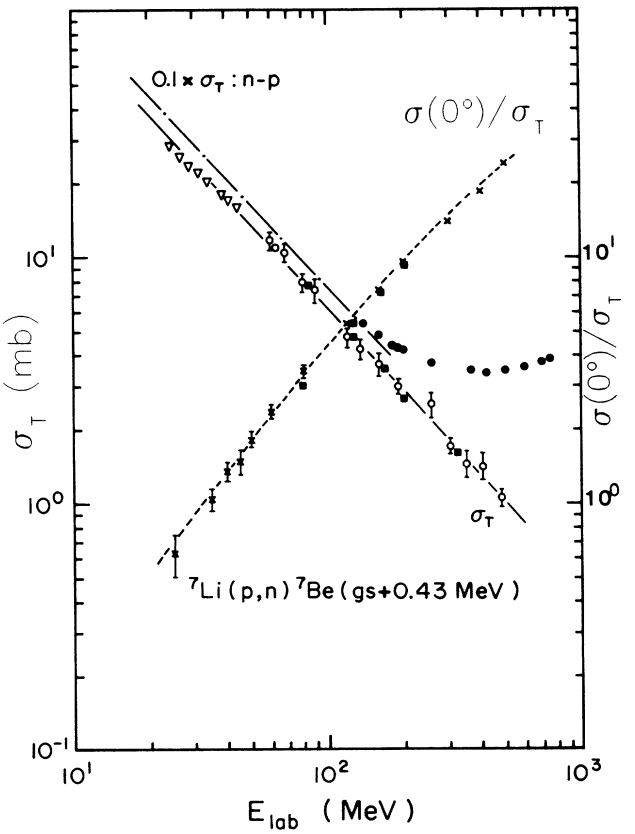

FIG. 8. Total cross section values for the ^{7}Li(p,n)^{7}Be (g.s.+0.43 MeV) reaction are shown versus proton energy. The dashed-dotted line represents values for the total free n-p elastic cross section divided by 10 in the 20–150 MeV energy range. Above 150 MeV the solid circles represent the total free n-p cross section divided by 10. The solid squares are calculated DWIA values (see text). The ratio between the differential zero degree ^{7}Li(p,n)^{7}Be (g.s.+0.43 MeV) cross section and the total cross section values are indicated by crosses joined by the dashed curve.

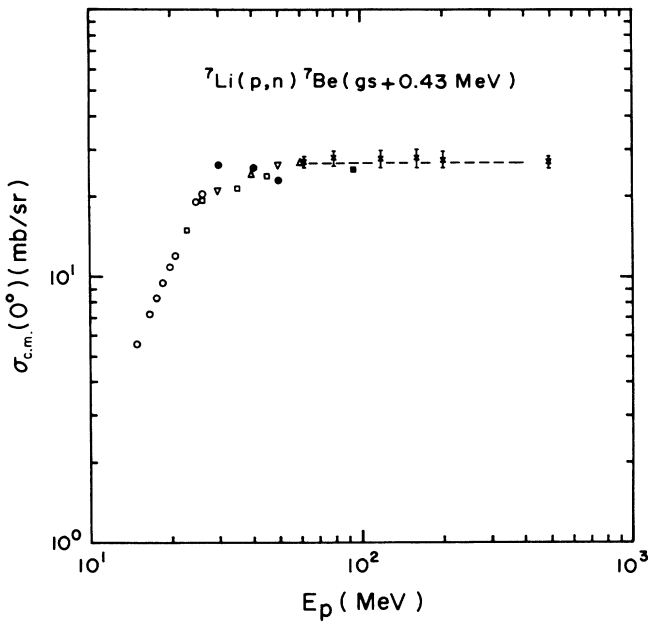

FIG. 9. Values for the zero degree differential cross section for the ^{7}Li(p,n)^{7}Be (g.s.+0.43 MeV) reaction are indicated versus proton energy. The dashed line represents the value 26.1 mb/sr from Ref. 12.

We also present in Fig. 8 the energy dependence of the ratio between the sum of the zero degree (p,n) differential cross section to the g.s. and 0.43 MeV state in ^{7}Be to the total cross section. The data points are indicated with crosses while DWIA calculations at 80, 120, 160, and 200 MeV are shown as solid squares. The data points up to about 160 MeV are well described by the equation

$$\ln[\sigma(0°)/\sigma_T] = 1.192 \ln E_p - 4.047 , \quad (15)$$

where E_p is in MeV and the cross sections are in mb. This relationship seems to be different above 200 MeV, when the data points reported by Watson *et al.*[12] at 200, 300, and 400 MeV and data from Ref. 48 at 500 MeV are included. The dashed line in Fig. 8 corresponds to Eq. (15) up to 160 MeV and has been extended to join the data points up to 500 MeV.

The zero degree differential center-of-mass cross sections for the ^{7}Li(p,n)^{7}Be (g.s.+0.43 MeV) transitions are presented in Fig. 9 for energies between 15 and 500 MeV. Taddeucci *et al.*[15] in a recent paper report on a detailed study of the zero degree cross section for these transitions in the energy range up to 790 MeV. The dotted line represents the value 26.1 mb/sr obtained as a weighted average in the 60–400 MeV energy range deduced by Watson *et al.*[12]

F. Comparison between (p,n), (n,p), and (p,p') cross sections on ^{6}Li

The nucleus ^{6}Li is a self-conjugate nucleus. As such the ^{6}Li(p,n)^{6}Be (g.s.) and the ^{6}Li(n,p)^{6}He (g.s.) cross sections are expected to be equal at the same bombarding energies, assuming an unbroken isospin symmetry. Similarly, the ^{6}Li(p,p')^{6}Li (3.56 MeV, 0^+, $T=1$) cross section at the same incident proton energy is simply related to the other two cross sections by a Clebsch-Gordan coefficient, which in this case has a value of 2. Thus it is expected that $\sigma_{p,n}=\sigma_{n,p}=2\sigma_{p,p'}$.

The ^{6}Li(n,p)^{6}Be (g.s.) reaction has been reported by Measday[60] at 150 MeV, by Pocanic *et al.*[9] at 120 MeV, and recently by Jackson[10] and Häusser[11] at 200 and 280 MeV. Values for the differential cross section to the g.s. transition plotted versus momentum transfer q are presented in Fig. 10. The solid curve represents the line through the ^{6}Li(p,n)^{6}Be (g.s.) data points from Fig. 2. The (p,p') differential cross section to the 3.56 MeV, 0^+, $T=1$ state has been studied at 136 MeV (Ref. 7) and at 200 MeV (Ref. 8). The (p,p') differential cross section values multiplied by two are also presented in Fig. 10. The values from Ref. 7 below $q=0.8$ fm^{-1} are much lower than those of Ref. 8 and those reported in Ref. 11. We do not know the reasons for that discrepancy.

The data seem to reflect a similar value for the extrapolated $q=0$ differential cross section indicating that each

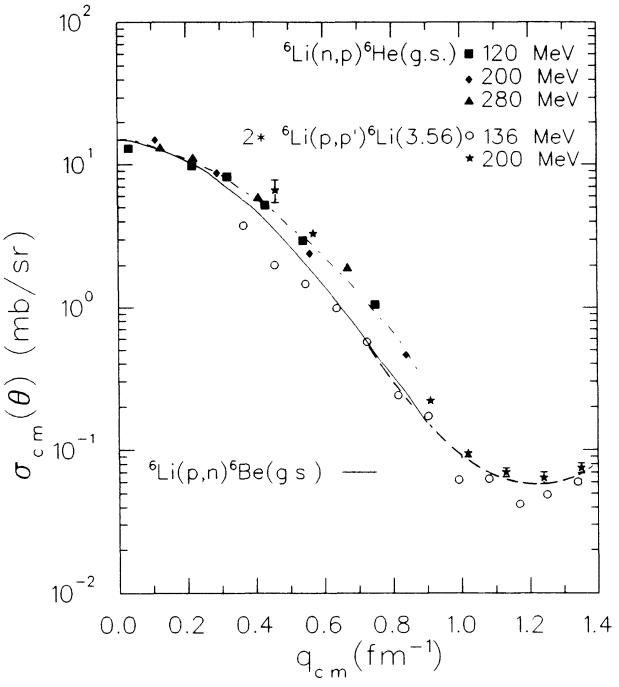

FIG. 10. The solid line represents the average value for the ^{6}Li(p,n)^{6}Be (g.s.) differential cross section versus momentum transfer (see Fig. 2). Values for the ^{6}Li(p,n)^{6}He (g.s.) and twice the values for the ^{6}Li(p,p')^{6}Li (3.56 MeV) differential cross sections are also shown. The dashed and dotted-dashed lines are just drawn to guide the eye through the (p,p') data points and the (n,p) data points, respectively.

one of these measurements lead to an equivalent B(GT) value. However, the angular distributions seem to have different shape. If the orbital contribution to the $M1$ transition observed in the ^{6}Li(p,p')^{6}Li (3.56 MeV) reaction plays a significant role, one would expect the differential angular distribution to be different from those for the analog charge-exchange reactions. However, angular distribution shapes for the (n,p) and (p,n) reaction should be similar. In the case of ^{12}C,[26] the ^{12}C(p,n)^{12}N (g.s.) transition and its analog, the ^{12}C(p,p')^{12}C (15.11 MeV) reaction, have the same angular distribution. The ^{12}C(n,p)^{12}B (g.s.) angular distribution at 200 MeV reported by Häusser[11] also seems to agree with the (p,n) and (p,p') results.

The present set of data indicates that the ^{6}Li(n,p)^{6}Be (g.s.) reaction and the ^{6}Li(p,p')^{6}Li (3.56 MeV) cross section display a very similar angular distribution. However, the ^{6}Li(p,n)^{6}Be (g.s.) transition shows lower cross section values in the $0.3 < q < 0.8$ fm^{-1} interval. Possible reasons for this difference may be attributed to the different radial distributions of the transition densities. The $A=6$ system has a low two-particle emission threshold and the ^{6}He (g.s.) and ^{6}Be (g.s.) wave functions may be quite different. This would also have consequences for heavy-ion-induced charge-exchange reactions.

V. CONCLUSIONS

We report the ^{6,7}Li(p,n)^{6,7}Be reactions measured for incident energies between 60 and 200 MeV. Particular attention is provided to the study of the differential angular distribution corresponding to GT and F transitions. We report the GT strength observed for these reactions up to 40 MeV excitation. The energy dependence of the $\sigma\tau$ and τ effective interactions is reported in this energy range, as well as the energy dependence of the total and zero degree differential cross sections for the ^{7}Li(p,n)^{7}Be (g.s. +0.43 MeV) transitions.

A value for the ^{7}Be beta decay branching ratio is derived from the measured ratio of (p,n) differential cross section to the g.s. and 0.43 MeV state in ^{7}Be. Finally, a comparison is presented for data reported for the (n,p), (p,p'), and (p,n) reactions in ^{6}Li populating isospin triplets.

ACKNOWLEDGMENTS

We wish to thank D. E. Bainum, M. B. Greenfield, T. P. Welch, T. Masterson, and T. E. Ward for their valuable help during the experimental setup and data acquisition. This work was supported in part by the National Science Foundation, the U.S. Department of Energy, and the Danish Natural Science Research Council.

[1] J. D. Anderson, C. Wong, and V. A. Madsen, Phys. Rev. Lett. **24**, 1074 (1970).

[2] R. R. Doering, L. E. Young, R. K. Bhowmik, S. M. Austin, S. D. Schery, and R. DeVito, Michigan State University Annual Report 1974–1976; see also *Proceedings of the International Conference on Nuclear Structure, Tokyo, 1977* (International Academic Printing, Japan, 1977), p. 487.

[3] S. M. Austin, L. E. Young, R. R. Doering, R. DeVito, R. K. Bhowmik, and S. D. Schery, Phys. Rev. Lett. **44**, 972 (1980).

[4] T. N. Taddeucci, J. Rapaport, D. E. Bainum, C. D. Goodman, C. C. Foster, C. Gaarde, J. Larsen, C. A. Goulding, D. J. Horen, T. Masterson, and E. Sugarbaker, Phys. Rev. C **25**, 1094 (1982).

[5] F. Petrovich, R. H. Howell, C. H. Poppe, S. M. Austin, and G. M. Crawley, Nucl. Phys. **A383**, 355 (1982).

[6] G. L. Moake, L. J. Gutay, R. P. Scharenberg, P. T. Debevec, and P. A. Quin, Phys. Rev. C **21**, 2211 (1980); G. L. Moake, Indiana University Cyclotron Facility Internal Report No. 79-2, 1979.

[7] R. S. Henderson, S. F. Collins, B. M. Spicer, G. G. Shute, V. C. Officer, D. W. Devins, D. L. Friesel, and W. P. Jones, Nucl. Phys. **A372**, 117 (1981).

[8] C. W. Glover, C. C. Foster, P. Schwandt, J. R. Comfort, J. Rapaport, T. N. Taddeucci, D. Wang, G. J. Wagner, J. Seubert, A. W. Carpenter, J. A. Carr, F. Petrovich, R. J. Philpott, and M. J. Threapleton, Phys. Rev. C (to be published).

[9] D. Pocanic, K. Wang, C. J. Martoff, S. S. Hanna, R. C. Byrd, C. C. Foster, D. L. Friesel, and J. Rapaport, Can. J. Phys. **65**, 687 (1987).

[10] K. P. Jackson and A. Celler in *Spin Observables of Nuclear Probes,* edited by C. J. Horowitz, C. D. Goodman, and G. E. Walker (Plenum, New York, 1988), p. 139; K. P. Jackson

et al., Phys. Lett. B **201**, 25 (1988).
[11]O. Häusser, INS Symposium on Nuclear Physics at Intermediate Energy, Tokyo, 1988, edited by T. Fukada and T. Nagal (World Scientific, Singapore, 1989).
[12]J. W. Watson *et al.*, Phys. Rev. C **40**, 22 (1989).
[13]T. E. Ward, C. C. Foster, G. E. Walker, J. Rapaport, and C. A. Goulding, Phys. Rev. C **25**, 762 (1982).
[14]J. D'Auria, M. Dombsky, L. Moritz, T. Ruth, G. Sheffer, T. E. Ward, C. C. Foster, J. W. Watson, B. D. Anderson, and J. Rapaport, Phys. Rev. C **30**, 1999 (1984).
[15]T. N. Taddeucci *et al.*, Phys. Rev. C (to be published).
[16]C. D. Goodman, C. C. Foster, M. B. Greenfield, C. A. Goulding, D. A. Lind, and J. Rapaport, IEEE Trans. Nucl. Sci. NS-**26**, 2248 (1979).
[17]C. D. Goodman and E. Kowalski, Indiana University Cyclotron Facility report, 1979 (unpublished).
[18]C. A. Goulding, M. B. Greenfield, C. C. Foster, T. E. Ward, J. Rapaport, D. E. Bainum, and C. D. Goodman, Nucl. Phys. **A331**, 29 (1979).
[19]C. Gaarde, J. Rapaport, T. N. Taddeucci, C. D. Goodman, C. C. Foster, D. E. Bainum, C. A. Goulding, M. B. Greenfield, D. J. Horen, and E. Sugarbaker, Nucl. Phys. **A369**, 258 (1981).
[20]F. Ajzenberg-Selove, Nucl. Phys. **A490**, 1 (1988).
[21]W. A. Fowler, Nature **238**, 24 (1972).
[22]V. M. Fetisov and Yu. S. Kopysov, Phys. Lett. **40B**, 602 (1972).
[23]D. M. Shoplik, J. J. Murphy II, and J. Asai, Phys. Rev. C **19**, 1144 (1979).
[24]L. W. Fagg, W. L. Bendel, N. Ensslin, and E. C. Jones, Jr., Phys. Lett. **44B**, 163 (1973).
[25]C. D. Goodman, C. A. Goulding, M. B. Greenfield, J. Rapaport, D. E. Bainum, C. C. Foster, W. G. Love, and F. Petrovich, Phys. Rev. Lett. **44**, 1755 (1980).
[26]J. Rapaport, T. N. Taddeucci, C. Gaarde, C. D. Goodman, C. C. Foster, D. Horen, E. Sugarbaker, T. G. Masterson, and D. Lind, Phys. Rev. C **24**, 335 (1981).
[27]J. L. Norton and P. Goldhammer, Nucl. Phys. **A165**, 33 (1971).
[28]S. Cohen and D. Kurath, Nucl. Phys. **73**, 1 (1965); Nucl. Phys. **A101**, 1 (1967); T.-S. H. Lee and D. Kurath, Phys. Rev. C **21**, 293 (1980).
[29]Y. W. Lui, O. Karban, A. K. Basak, C. O. Blyth, J. M. Nelson, and S. Roman, Nucl. Phys. **A297**, 189 (1978).
[30]R. Schaeffer and J. Raynal, Code DWBA-70 (unpublished).
[31]B. Goeffrion, N. Marty, M. Morlet, B. Tatischeff, and A. Willis, Nucl. Phys. **A116**, 209 (1968).
[32]G. L. Moake and P. T. Debevec, Phys. Rev. C **21**, 25 (1980).
[33]N. Hutcheon, Nucl. Phys. **A154**, 261 (1970).
[34]J. R. Comfort and B. C. Karp, Phys. Rev. C **21**, 2162 (1980).
[35]W. G. Love and M. Franey, Phys. Rev. C **24**, 1073 (1981).
[36]H. V. von Geramb, in *The Interaction Between Medium Energy Nucleons in Nuclei,* AIP Conf. Proc. No. 97, edited by H. O. Meyer (AIP, New York, 1983), p. 44.
[37]M. Lacombe, B. Loiseau, J. M. Richard, R. Vinh Mau, J. Coté, P. Pirés, and R. de Tourreil, Phys. Rev. C **21**, 861 (1980).
[38]See papers by W. G. Love, F. Petrovich, and C. D. Goodman, in *The (p,n) Reaction and the Nucleon-Nucleon Interaction,* edited by C. D. Goodman, S. M. Austin, S. D. Bloom, J. Rapaport, and G. R. Satchler (Plenum, New York, 1980), pp. 23, 115, and 149.
[39]T. N. Taddeucci, C. A. Goulding, T. A. Carey, R. C. Byrd, C. D. Goodman, C. Gaarde, J. Larsen, D. Horen, J. Rapaport, and E. Sugarbaker, Nucl. Phys. **A469**, 125 (1987).
[40]D. H. Wilkinson, Nucl. Phys. **A377**, 474 (1982); see also P. Bopp, D. Dubbers, L. Hornig, E. Klemt, J. Last, H. Schütze, S. J. Freedman, and O. Scharpf, Phys. Rev. Lett. **56**, 919 (1986).
[41]F. Ajzenberg-Selove and T. Lauritsen, Nucl. Phys. **A227**, 1 (1974).
[42]F. Ajzenberg-Selove, Nucl. Phys. **A320**, 1 (1979).
[43]J. Rapaport, Can. J. Phys. **65**, 574 (1987).
[44]C. D. Goodman, R. C. Byrd, I. J. Van Heerden, T. A. Carey, D. J. Horen, J. S. Larsen, C. Gaarde, J. Rapaport, T. P. Welch, E. Sugarbaker, and T. N. Taddeucci, Phys. Rev. Lett. **54**, 877 (1985).
[45]J. W. Watson, W. Pairsuwan, B. D. Anderson, A. R. Baldwin, B. S. Flanders, R. Madey, R. J. McCarthy, B. A. Brown, B. H. Wildenthal, and C. C. Foster, Phys. Rev. Lett. **55**, 1369 (1985).
[46]T. N. Taddeucci, in *Spin Observables of Nuclear Probes,* edited by C. J. Horowitz, C. D. Goodman, and G. E. Walker (Plenum, New York, 1988), p. 425.
[47]W. G. Love, K. Nakayama, and M. A. Franey, Phys. Rev. Lett. **59**, 1401 (1987); K. Nakayama and W. G. Love, Phys. Rev. C **38**, 51 (1988).
[48]J. Rapaport *et al.*, Phys. Rev. C **39**, 1929 (1989).
[49]John N. Bahcall, *Neutrino Astrophysics* (Cambridge University Press, Cambridge, Masschusetts, 1989).
[50]H. P. Trautvetter, H. W. Becker, L. Buchmann, J. Gorres, K. U. Kettner, C. Rolfs, P. Schmalbrock, and A. E. Vlieks, Ver. Dtsch. Phys. Ges. **VI**, 1141 (1983).
[51]R. T. Skelton and R. W. Kavanagh, Nucl. Phys. **A414**, 141 (1984).
[52]M. Martin, Nuclear Data Group, private communication.
[53]T. N. Taddeucci, C. D. Goodman, R. C. Byrd, T. A. Carey, D. J. Horen, J. Rapaport, and E. Sugarbaker, Nucl. Instrum. Methods A **241**, 448 (1985).
[54]L. P. Robertson, R. C. Hanna, K. Ramavataram, D. W. Devins, T. A. Hodges, and Z. T. Moroz, Nucl. Phys. **A134**, 545 (1969).
[55]R. Henneck, C. Gysin, P. Haffler, M. Hammans, W. Lorenzon, M. A. Pickar, and I. Sick, Phys. Rev. C **37**, 2224 (1988).
[56]H. Sakai *et al.*, in *Antinucleon and Nucleon-Nucleus Interactions,* edited by G. E. Walker, C. D. Goodman, and C. Olmer (Plenum, New York, 1985), p. 293.
[57]T. N. Taddeucci, Can. J. Phys. **65**, 557 (1987).
[58]S. D. Schery, L. E. Young, R. R. Doering, S. M. Austin, and R. K. Bhowmik, Nucl. Instrum. Methods **147**, 399 (1977).
[59]R. A. Arndt, J. S. Hyslop, and L. D. Roper, Phys. Rev. D **35**, 128 (1987).
[60]D. Measday, Phys. Rev. **161**, 1071 (1967).